Shi et al. Earth, Planets and Space 2014, 66:30
http://www.earth-planets-space.com/content/66/1/30

Earth, Planets and Space
a SpringerOpen Journal

FULL PAPER Open Access

Local troposphere augmentation for real-time precise point positioning

Junbo Shi[1*], Chaoqian Xu[1], Jiming Guo[1] and Yang Gao[2,3]

Abstract

The IGS real-time service (RTS) enables real-time precise point positioning (PPP) at a global scale. A long convergence time however is still a challenging factor. In order to reduce the convergence time, external troposphere corrections could be introduced to remove the troposphere effects on the coordinate solution. This paper proposes the use of a local troposphere model to augment real-time PPP. First, undifferenced observations from a network of multiple stations are processed to estimate the station-based troposphere zenith wet delay (ZWD). A set of local troposphere fitting coefficients are then derived using a proposed optimal fitting model. Finally, the determined troposphere fitting coefficients are broadcast to users to reduce the convergence time in the user solution. A continuous operating reference station (CORS) network is utilized to assess the performance of the proposed approach under quiet and active troposphere conditions. The numerical results show that the overall fitting precisions of the local troposphere model can reach 1.42 and 1.05 cm under the two troposphere conditions. The convergence time of the positioning solutions, especially the height solution, can be greatly reduced using the local troposphere model. The horizontal accuracy of 9.2 cm and the vertical accuracy of 10.1 cm are obtainable under the quiet troposphere condition after 20 min of initialization time, compared to the 14.7 cm horizontal and 21.5 cm vertical accuracies in the conventional troposphere estimation approach. Moreover, the horizontal accuracies of 13.0 cm and the vertical accuracies of 12.4 cm have also been obtained after 20 min under the active troposphere condition.

Keywords: Real-time precise point positioning; Local troposphere augmentation; Optimal fitting model; Convergence time

Background

Investigations on real-time satellite orbit and clock products for real-time precise point positioning (PPP) began about one decade ago. Gao and Chen (2004) carried out the performance analysis of PPP using Jet Propulsion Laboratory (JPL)'s real-time orbit and clock corrections for static and kinematic applications. The obtainable positioning accuracies are comparable to those using International Global Navigation Satellite System (GNSS) Service (IGS) final orbit and clock products that however are available with at least 17-h latency (Kouba 2009). Tao (2008) investigated the performance of PPP-inferred troposphere estimates using JPL's real-time products and concluded that the obtained real-time PPP-inferred zenith wet delay had an accuracy of approximately 13 mm. In 2007, IGS initiated the real-time pilot project (RTPP) with the infrastructure of real-time GNSS data streams on a global basis. Based on the real-time GNSS observations, several real-time orbit and clock products are generated by participating IGS RTPP agencies. Using BKG's real-time corrections, Altiner et al. (2010) demonstrated a horizontal accuracy of 10 cm and a vertical accuracy of 20 cm for real-time PPP with 17-h observations at station CONZ. As to the convergence time, 10 min were found sufficient to achieve 10-cm horizontal accuracy at station FFMJ. A bias of 40 cm, however, was identified in the vertical solution. Sturze et al. (2012) demonstrated a horizontal accuracy of 4 to approximately 5 cm after convergence based on daily solutions from six participating IGS RTPP agencies. Wang et al. (2013) assessed the near real-time PPP-inferred troposphere parameter, using Centre National d'Etudes Spatiales (CNES)'s real-time corrections, and found a mean bias of approximately 6.5 mm and a root mean square (RMS) error of approximately 13 mm for the zenith wet delay compared to those using post-mission products.

* Correspondence: jbshi@sgg.whu.edu.cn
[1]School of Geodesy and Geomatics, Wuhan University, Wuhan 430079, China
Full list of author information is available at the end of the article

Using a satellite-difference and epoch-difference method, Li et al. (2010) and Chen et al. (2013) demonstrated a horizontal accuracy of 5 cm using hourly observations in the static mode and 3D precision of 10 cm after 20-min convergence time in the kinematic mode. After the 6-year experimental tests, IGS officially announced the real-time service (RTS) on 1 April 2013, which provides Global Positioning System (GPS) real-time orbit and clock corrections and experimental GLONASS corrections to support real-time PPP at a global scale (Caissy et al. 2012).

Although IGS RTS has solved the latency issue of precise satellite orbit and clock products, the long convergence time still remains a challenging factor for real-time PPP. In fact, the PPP convergence highly depends on the estimation of the troposphere delays. Therefore, regional troposphere models have been studied to reduce the convergence time for (near) real-time PPP. Ibrahim and EI-Rabbany (2011) evaluated the numerical weather prediction based on the National Oceanic and Atmospheric Administration (NOAA) tropospheric signal delay model within the North America. The results demonstrate that the PPP convergence using the NOAA troposphere model can be improved by 1%, 10%, and 15% for latitude, longitude, and height components, respectively, compared to that using the Hopfield model. Hadas et al. (2013) assessed the benefits of near real-time regional troposphere model for PPP. The IGS's ultra-rapid orbit and clock products are used to generate the near real-time regional troposphere model which greatly improves the height accuracy in simulated real-time PPP scenarios. Li et al. (2011) investigated the regional atmosphere augmentation for real-time PPP with instantaneous ambiguity resolution. Li's method however requires the user to send approximate coordinates to the server in order to receive an interpolated troposphere delay from the server. Such two-way communication mode would increase the user's communication cost and limit the server's maximum number of allowed connections.

A real-time troposphere augmentation method is proposed in this paper to eliminate the limitation of the maximum number of allowed users and reduce the convergence time of real-time PPP. We first utilize the IGS real-time orbit and clock corrections to estimate the station-based troposphere zenith wet delays based on a continuous operating reference station (CORS) network. A novel method is then proposed to determine the fitting coefficients of the optimal local troposphere model which does not require the user's approximate coordinates and can be broadcast to unlimited users. Since this approach is based on the one-way communication mode, it eliminates the need for users to communicate with the server and also has no limit on the number of allowed users.

The paper will be organized as follows. The Section 'Methods' describes the flowchart and the mathematics of the proposed local troposphere augmentation for real-time PPP. Section 'Results and discussion' analyzes two GPS daily observations under quiet and active troposphere conditions in terms of the accuracy of IGS real-time orbit and clock products, the precisions of the local troposphere model, and the benefits of local troposphere augmentation to real-time PPP. Finally, some conclusion remarks and future works are given in Section 'Conclusions.'

Methods

Figure 1 shows the flowchart that describes the proposed real-time local troposphere model determination at the server end and the real-time PPP with local troposphere augmentation at the user end. For the determination of the real-time local troposphere model, the IGS real-time orbit and clock corrections are needed at each reference station to perform real-time PPP which estimates four types of parameters: the coordinates, the receiver clock error, the troposphere delay, and the ambiguity parameters. As the troposphere zenith hydrostatic delay (ZHD) can be corrected using the global pressure and temperature (GPT) model and the Saastamoinen model (Boehm et al. 2007; Gérard and Luzum 2010), the estimated troposphere parameter is the troposphere zenith wet delay (ZWD). The station-based ZWD values of the reference stations are utilized to determine a set of optimal troposphere ZWD fitting coefficients which are then broadcast to the user. The user needs to calculate the ZWD value based on its geographic location and the received troposphere ZWD fitting coefficients. In order to maximize the performance, the ZHD at the user end must also be corrected using the GPT and Saastamoinen models as those used at the server end. The calculated ZWD is then applied to remove the residual troposphere delay at the user end. As a result, real-time PPP at the user end only needs to estimate three types of parameters: the coordinates, the receiver clock error, and the ambiguities.

The methods for determining a local troposphere model can be classified into two categories. The first category requires the user to send its approximate coordinates to the server and receive the interpolated troposphere delay from the server in a two-way communication manner. One implementation is the virtual reference station (VRS) technology (Alves and Monico 2011). Dai et al. (2004) summarized the equivalence of the different troposphere interpolation methods requiring the two-way communication connection. On the other hand, if a set of local troposphere fitting coefficients could be broadcast from the server to the user, then there is no need for the user to communicate with the server and the maximum number of allowed users becomes unlimited. Xiong et al. (2006)

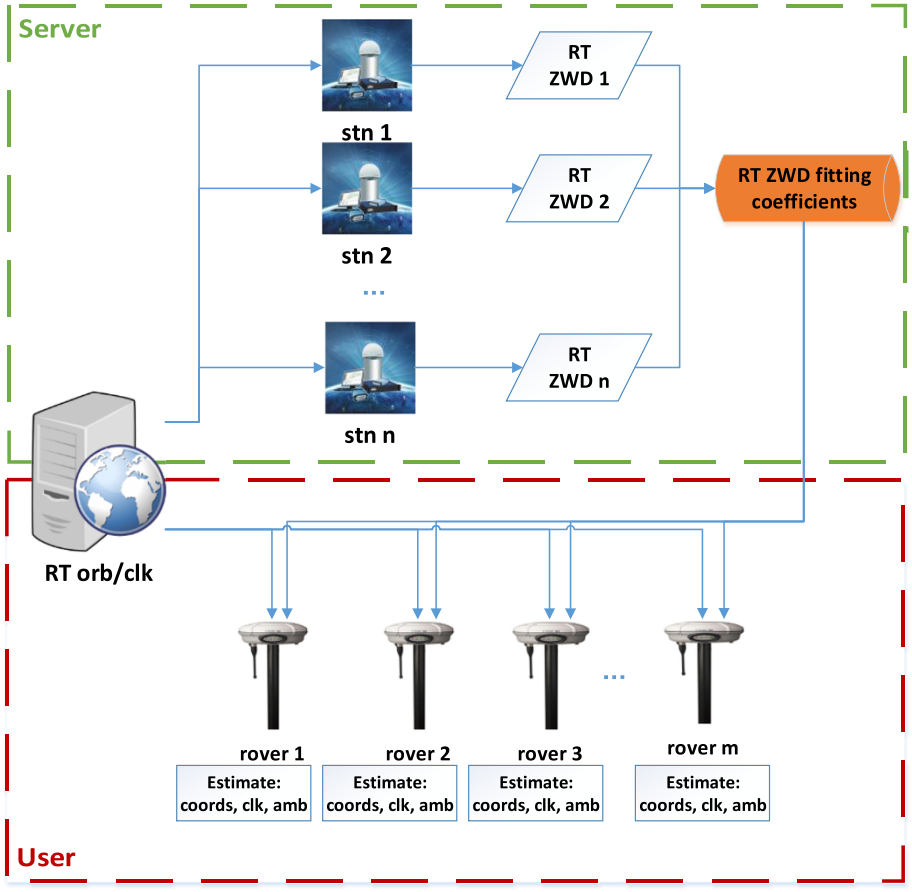

Figure 1 Flowchart of the local troposphere augmentation for real-time (RT) PPP. The server end (top green box) determines the real-time ZWD fitting coefficients which are broadcast to the users. The user end (bottom red box) utilizes the real-time orbit/clock corrections and the real-time ZWD fitting coefficients to perform real-time PPP with local troposphere augmentation.

and Zhang et al. (2013) investigated the local troposphere model determination using several empirical fitting functions. Although the user communication cost has been eliminated and the maximum number of allowed users becomes unlimited, whether the utilized empirical fitting functions were optimal has not been investigated.

This paper proposes a method to determine the optimal fitting coefficients for local troposphere modeling. The general form of the second-order fitting model consists of the observation equations

$$\begin{aligned} \mathrm{ZWD}_i = {} & a_0 + a_1 x_i + a_2 y_i + a_3 h_i + a_4 x_i y_i \\ & + a_5 x_i h_i + a_6 y_i h_i + a_7 {x_i}^2 + a_8 {y_i}^2 \\ & + a_9 {h_i}^2 (i = 1, \ldots, n) \end{aligned} \tag{1}$$

and the constraint equations

$$0 = \varphi_j a_j (j = 0, \ldots 9) \tag{2}$$

where n denotes the number of reference stations, the subscript i denotes the index of the reference stations, ZWD_i is the troposphere zenith wet delay at the ith station, (x_i, y_i) are the Gaussian projection horizontal coordinates; h_i is the ellipsoid height; $(a_0, a_1, \ldots, a_9)$ are ten fitting coefficients; the subscript j denotes the index of the constraint coefficients; $\phi_j \in \{0, 1\}$ is the constraint coefficient of a_j.

The key to determining the optimal local troposphere model is to compute the optimal fitting coefficients. Unlike the previous work using empirical fitting functions, the optimal local troposphere model is always expressed as (1) with one set of ten fitting coefficients $(a_0, a_1, \ldots, a_9)$ satisfying the user-defined optimization criterion. The determination of the optimal fitting coefficients is described as follows. In step I, no constraint equation is constructed. The number of the constraint equation candidates is $C_{10}^0 = \frac{10!}{0!*(10-0)!} = 1$. Then only n observation Equation 1 is used to estimate the set of fitting coefficients $(a_0, a_1, \ldots, a_9)$ in a least-square estimator. In step II, one constraint equation is constructed. The number of the constraint equation candidates is $C_{10}^1 = \frac{10!}{1!*(10-1)!} = 10$. We can form ten combinations of one constraint

Equation 2 and n observation Equation 1 which are then used to estimate ten sets of fitting coefficients $(a_0, a_1, \ldots, a_9)$. In step III, two constraint equations are constructed. The number of the constraint equation candidates is $C_{10}^2 = \frac{10!}{2!*(10-2)!} = 45$. We can form 45 combinations of two constraint Equation 2 and n observation Equation 1 which are then used to estimate 45 sets of fitting coefficients $(a_0, a_1, \ldots, a_9)$. In step IV, we increment the size of constraint equations by 1 until the size increases to 10. The total number of the fitting coefficients sets is $\sum_{k=0}^{10} C_{10}^k = 1,024$. In step V, an optimization criterion is defined such as the minimization of the sum of square (SOS) of the troposphere fitting errors at n reference stations. The set of the fitting coefficients meeting the optimization criterion is determined as the optimal fitting coefficients for local troposphere modeling.

Note that in order to determine the optimal second-order local troposphere model with ten fitting coefficients, a minimum of ten reference stations are required. If the number of reference stations is less than 10, we can remove several fitting coefficients from Equation 1. For example, if we have nine reference stations and the height distribution of these reference stations is relatively smooth, we can remove the height-dependent coefficients (a_3, a_5, a_6, a_9) and keep only the horizontal-dependent coefficients $(a_0, a_1, a_2, a_4, a_7, a_8)$.

Using the general fitting model (Equations 1 and 2) and defining the optimization criterion, the optimal fitting coefficients can be obtained and broadcast to the users. With the user's approximate coordinates (x_i, y_i, h_i) and the received fitting coefficients $(a_0, a_1, \ldots, a_9)$, the troposphere ZWD at the user end can be computed by Equation 1.

Results and discussion

In this section, the datasets and the processing strategies used to evaluate the proposed method are first described. Two case studies concerning quiet and active troposphere conditions are analyzed afterwards to assess the performance of real-time PPP by local troposphere augmentation.

Data description and processing strategy

Two GPS daily observations with quiet and active troposphere conditions are processed based on a CORS network of nine stations shown in Figure 2. The longest distance is 191 km between no. 3 and no. 7, while the shortest distance is 18 km between no. 2 and no. 6. The maximum height difference is 26 m between no. 3 and no. 5. GPS observations are collected at the sampling interval of 30 s.

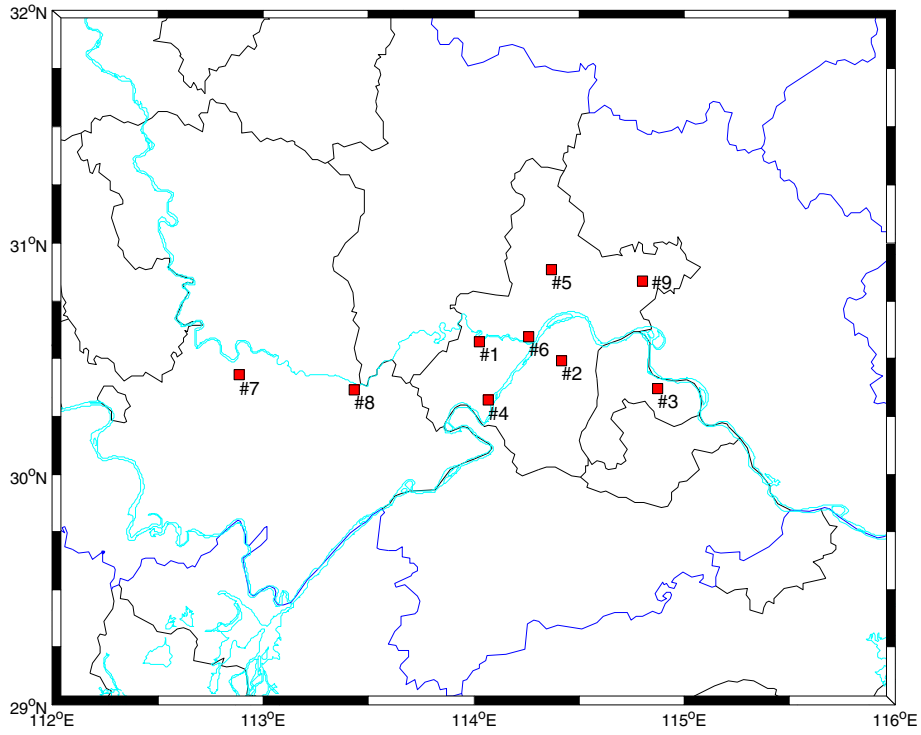

Figure 2 A CORS network. The network consists of nine stations with maximum distance of 191 km (no. 3 to no. 7) and maximum height difference of 26 m (no. 3 to no. 5).

In this paper, we concern two different situations with quiet and active troposphere conditions on the day of year (DOY) 2013 127 and 185, respectively. The weather condition on DOY 127 is relatively stable compared with those on the preceding and following days. A severe rainfall event, however, occurred on the following days of DOY 185, indicating an accumulating phase of the troposphere ZWD on DOY 185. For each case study, we first evaluate the accuracies of the real-time satellite orbit and clock products. The determination of the optimal ZWD fitting coefficients are then explained, followed by an assessment of the performance improvements of the real-time PPP with local troposphere augmentation over the conventional troposphere estimation approach. PPP software package used in this paper is P^3 developed by the Positioning and Mobile Information Systems Group of Department of Geomatics Engineering at The University of Calgary (Gao 2005) with some general processing settings summarized in Table 1. It should be noted that although we use real-time satellite corrections, the experiments are implemented in a simulated real-time mode. However, it will not reduce the general applicability and performance of the real-time PPP.

Case study 1: quiet troposphere condition

Real-time satellite orbit and clock corrections

In addition to the IGS combined correction stream, orbit and clock correction streams from several participating IGS RTS agencies are also provided for special considerations. For example, GFZ has been hosting a real-time PPP project with local reference network augmentation (Li et al. 2011); CNES has been developing a real-time zero-difference PPP integer ambiguity resolution demonstrator (Laurichesse 2011). Therefore, real-time PPP users can choose the proper correction stream to match their specific application. In this paper, the real-time correction stream from CNES with IGS mount-point ID CLK90 is selected because of its potential to support real-time PPP with integer ambiguity resolution. In this subsection, we will evaluate the accuracy of CNES real-time orbit and clock corrections which will be used for the determination of local troposphere model at the server end and the real-time PPP with local troposphere augmentation at the user end.

In order to obtain the precise satellite coordinates, an initial coordinate vector r and the velocity vector $\dot{r}$ should be first calculated based on the broadcast ephemeris. Then, the IGS real-time orbit corrections encoded as the Radio Technical Commission for Maritime Services (RTCM) space state representative (SSR) messages (RTCM Special Committee 104 2011) are applied to the initial coordinate vector by

$$r_{\mathrm{SSR}} = r - \left[e_{\mathrm{radial}} e_{\mathrm{along}} e_{\mathrm{cross}}\right] \delta O \tag{3}$$

where r_{SSR} is the corrected coordinate vector; $e_{\mathrm{radial}} = \frac{\dot{r}}{|\dot{r}|}$, $e_{\mathrm{along}} = \frac{r \times \dot{r}}{|r \times \dot{r}|}$, $e_{\mathrm{cross}} = e_{\mathrm{radial}} \times e_{\mathrm{along}}$; δO is the SSR orbit correction vector in radial, along, and cross-track components.

As to the precise satellite clock error, the application of SSR clock correction is represented by

$$dt^s{}_{\mathrm{SSR}} = dt^s + \frac{\delta C}{c} \tag{4}$$

where dt^s_{SSR} is the corrected satellite clock error; $\delta C = C_0 + C_1(t - t_0) + C_2(t - t_0)^2$ is the clock correction; t is the broadcast clock time; t_0 is the reference time obtained from SSR clock correction messages; C_0, C_1, C_2 are three clock correction coefficients in the SSR clock correction messages; c is the speed of light in vacuum.

One-day CNES real-time orbit and clock corrections are collected on DOY 127 to conduct the accuracy evaluation. The IGS 15-min final orbit and 30-s final clock products are used as reference. Lagrange interpolation is applied for the orbit product to match the GPS observations at 30 s interval. The orbit accuracy for each satellite is expressed as the RMS error of the differences between the calculated

Table 1 Processing settings for the troposphere estimation and augmentation approaches

	Troposphere estimation	Troposphere augmentation
Pressure and temperature data	GPT	GPT
Troposphere ZHD	Saastamoinen	Saastamoinen
Troposphere mapping function	Global mapping function (Boehm et al. 2006)	Global mapping function (Boehm et al. 2006)
Troposphere ZWD	Estimation	Local augmentation
Estimated parameters and initial standard deviations	Coordinates (10° m)	Coordinates (10° m)
	Receiver clock error (10^5 m)	Receiver clock error (10^5 m)
	Phase ambiguity (10^2 m)	Phase ambiguity (10^2 m)
	Troposphere ZWD (10^{-2} m)	
Estimator	Kalman filter	Kalman filter

coordinates and the reference coordinates. As to the clock's accuracy, a reference satellite is first selected to make a single difference with the other satellites in order to remove the clock datum inconsistency between the CNES real-time and IGS final clock products. In this paper, GPS PRN no. 1 is chosen as the reference satellite. The satellite clock accuracy is calculated as the RMS error of the differences between the calculated single-differenced clocks and the reference clocks.

Figures 3 and 4 illustrate the RMS accuracies of broadcast and SSR-corrected orbits and clocks with respect to the IGS final products on DOY 2013 127. Obviously, the orbit accuracies with SSR corrections (0.025/0.025/0.025 m in XYZ directions) are much better than the orbit accuracies without corrections (0.839/0.798/0.798 m in XYZ directions). As to the SSR-corrected clocks, an overall accuracy of 0.441 ns is obtained while that for the broadcast clocks is 3.085 ns.

Determination of optimal local troposphere fitting coefficients

CNES real-time orbit and clock corrections are applied to conduct real-time PPP-inferred troposphere estimation at the reference stations. The *a priori* troposphere zenith hydrostatic delay is calculated based on GPT-derived climatological data and Saastamoinen model. The residual troposphere zenith wet delay is estimated in a random walk pattern. Other processing settings are the same as those for the troposphere estimation approach listed in Table 1.

As the number of the reference stations is less than 10, the general second-order fitting model cannot be conducted. We remove the second-order terms from Equations 1 and 2 to perform the general first-order fitting model which only considers four fitting coefficients (a_0, a_1, a_2, a_3):

$$ZWD_i = a_0 + a_1 x_i + a_2 y_i + a_3 h_i \tag{5}$$

The troposphere ZWD values are chosen at the interval of 30 min between UTC 02:00 and 22:00 so that 42 samples are available for each station. At each sampling epoch, we use eight troposphere ZWD values to determine the troposphere fitting coefficients and interpolate the troposphere zenith wet delay $ZWD_{\text{interpolated}}$ for the ninth station. The interpolated troposphere delay is then utilized to evaluate the precision of the local troposphere model along with the estimated troposphere zenith wet delay $ZWD_{\text{estimated}}$. The optimum criterion is defined as

$$\sqrt{\sum_{j=1}^{9}\left(\sum_{i=1}^{42}\left(ZWD_{\text{estimated}} - ZWD_{interpolated}\right)_{ij}^{2}/42\right)} = \min \tag{6}$$

According to the optimum criterion (6), the optimum local troposphere fitting coefficients for the test network are determined with a SOS value of 1.42 cm. The

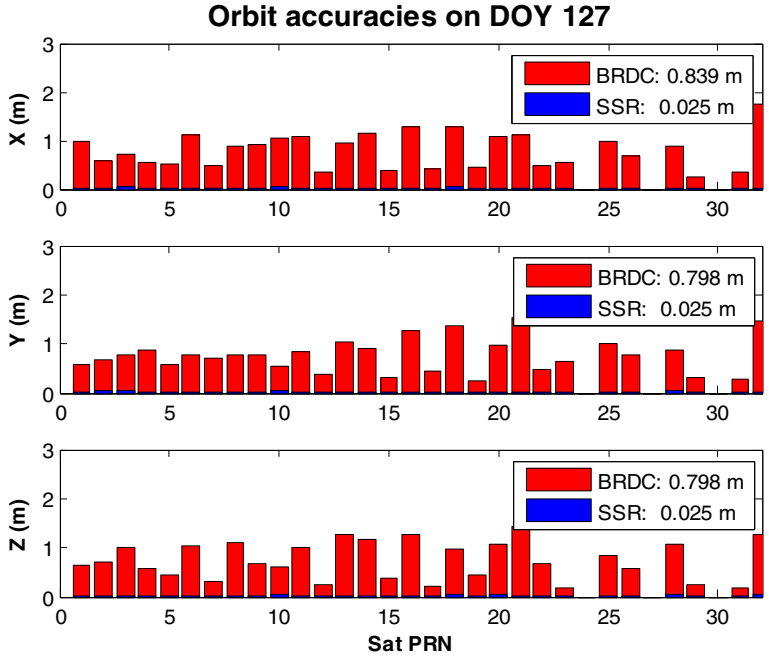

Figure 3 RMS accuracies of BRDC and SSR-corrected orbits against IGS final orbit products on DOY 2013 127.

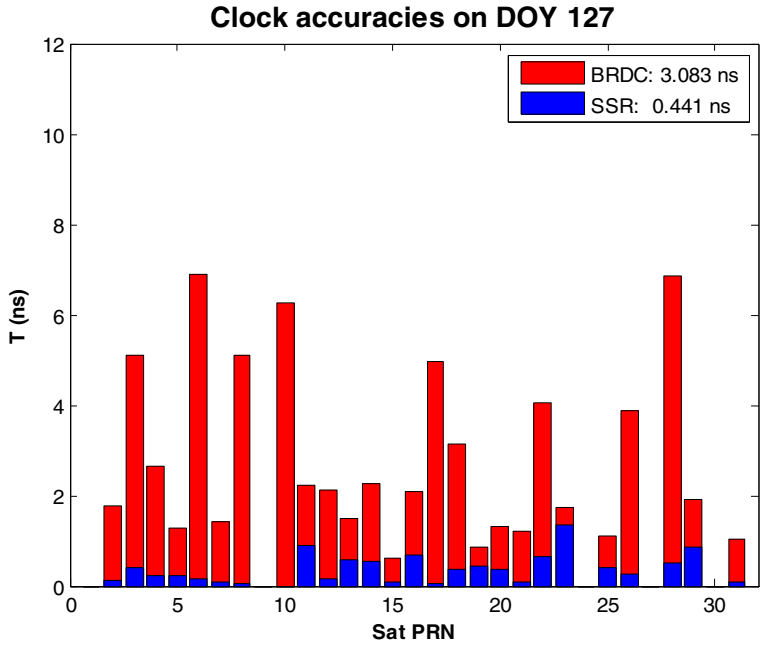

Figure 4 RMS accuracies of BRDC and SSR-corrected clocks against IGS final clock products on DOY 2013 127.

troposphere ZWD fitting precisions for each station are listed in Table 2. The interpolated ZWD series at station no. 5 are taken as an example in Figure 5. For the purpose of comparison, the estimated ZWD values at station no. 5 are also illustrated. The interpolated ZWD values match the estimated ZWD values quite well with a maximum discrepancy of approximately 3 cm and an average discrepancy of 1.55 cm.

Real-time PPP with local troposphere augmentation

To evaluate the performance of real-time PPP by local troposphere augmentation, we split the daily observations into 2-h data sets for the test stations. A total number of 90 2-h datasets are obtained and have been processed using the CNES real-time corrections described in subsection 'Real-time satellite orbit and clock corrections.' The local troposphere model has also been determined in subsection 'Determination of optimal local troposphere fitting coefficients.' The troposphere ZHD is corrected by the GPT and Saastamoinen models, whereas the troposphere ZWD is corrected by the interpolated ZWD based on the local troposphere fitting coefficients so that no troposphere estimation is needed at the user end. All other settings can be found as the troposphere augmentation approach in Table 1.

Table 2 Precision of the local troposphere model for each station in case 1

Site	Station number									Overall
	1	2	3	4	5	6	7	8	9	
RMS (cm)	0.85	0.59	2.09	0.90	1.55	1.98	1.20	1.27	1.62	1.42

Figure 6 demonstrates the north/east/up coordinate solutions with troposphere estimation and augmentation during UTC 18:00 and 20:00 of station no. 5 as an example. The two horizontal coordinate solutions with troposphere augmentation converge slightly faster than those with troposphere estimation. On the other hand, the convergence of the vertical solution is significantly improved using the local troposphere augmentation. When the troposphere parameter is estimated, the height solution converged after 1 h, but it requires only about 15 min with local troposphere augmentation.

Although the improvements by the local troposphere augmentation as shown in Figure 6 are found significant, the satellite geometry during the observation period is also an important factor which would affect the convergence of real-time PPP. Therefore, we apply the same processing strategy used for station no. 5 to the rest sessions and the rest stations. Given in Figures 7 and 8 are the horizontal and vertical positioning RMS accuracies after three selected initialization periods, namely 20, 60, and 100 min. The horizontal RMS accuracy after 20 min is 13.7 cm with troposphere estimation whereas it reduces to 9.4 cm when the local troposphere augmentation is applied. A longer initialization time of 60 or 100 min, however, does not bring significant improvements as the horizontal RMS

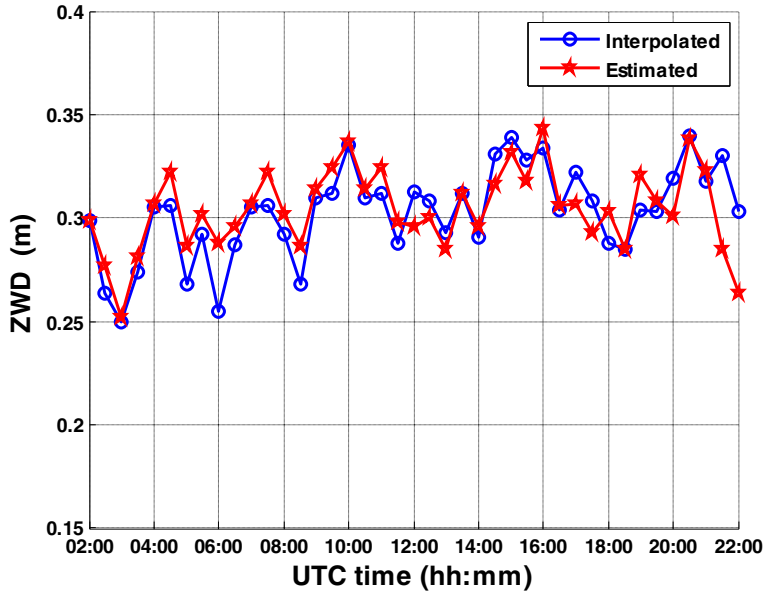

Figure 5 Interpolated and estimated ZWD. Interpolated (blue circle) and estimated (red star) ZWD at station no. 5 from UTC 02:00 to 22:00 on DOY 127.

accuracy differs slightly (i.e., 7.5 versus 5.6 cm or 6.4 versus 5.3 cm). As for the height solution, the RMS accuracy is improved from 18.3 to 10.1 cm after the 20-min initialization time, a much more significant improvement than the horizontal counterpart. It can also be seen from Figure 8 that there is still an approximately 10-cm bias for the height solutions with local troposphere augmentation. This bias is mainly caused by the discrepancy between the estimated and interpolated troposphere ZWD listed in Table 2. In summary, the local

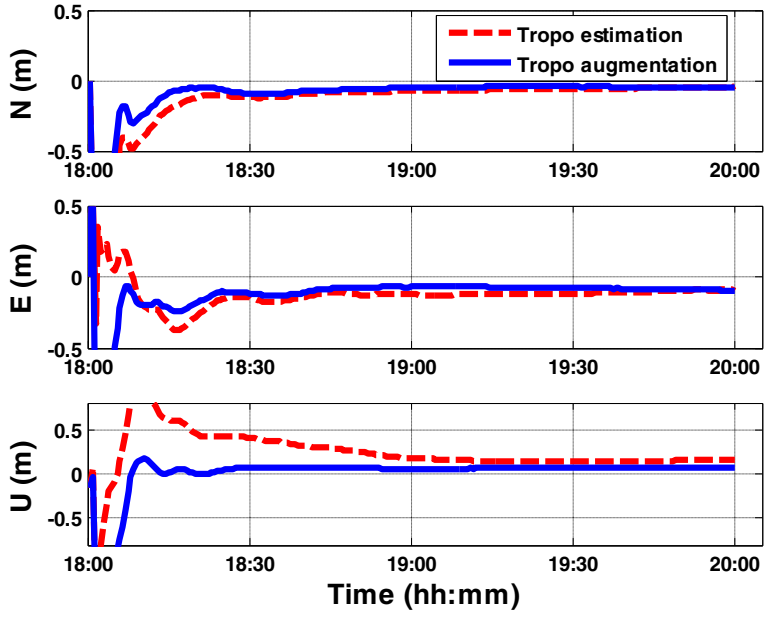

Figure 6 Real-time PPP positioning solutions of station no. 5. With troposphere estimation (red dotted line) and augmentation (blue solid line) from UTC 18:00 to 20:00.

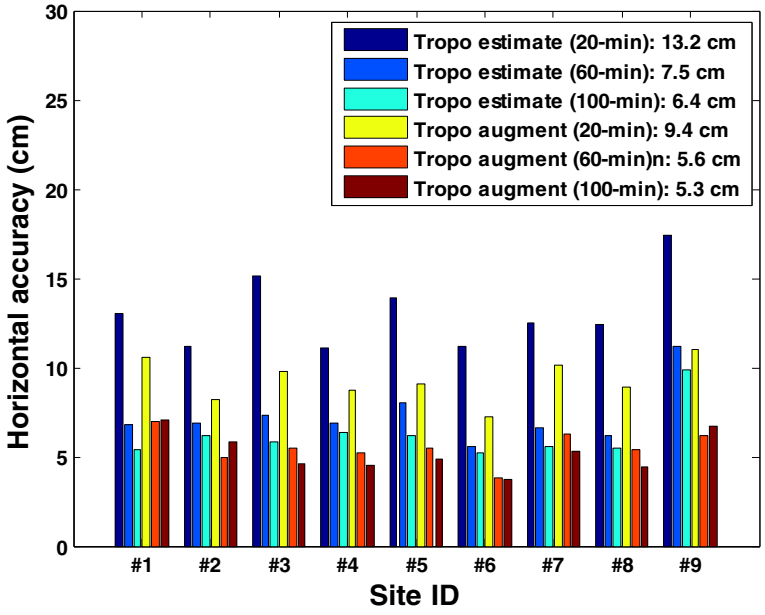

Figure 7 Horizontal RMS accuracies with troposphere estimation and augmentation on DOY 127. Horizontal RMS accuracies with troposphere estimation and augmentation after 20-, 60-, and 100-min initialization periods.

troposphere model can augment real-time PPP in terms of positioning accuracy and convergence by eliminating the troposphere effects on the coordinate solution. However, the positioning accuracies are still limited by other factors including the satellite geometry and ambiguity fractional biases which cannot be corrected by the local troposphere model. To further improve the positioning performance as shown in Figures 7 and 8, the integer phase ambiguity resolution technique should be considered in the future for real-time PPP with local troposphere augmentation.

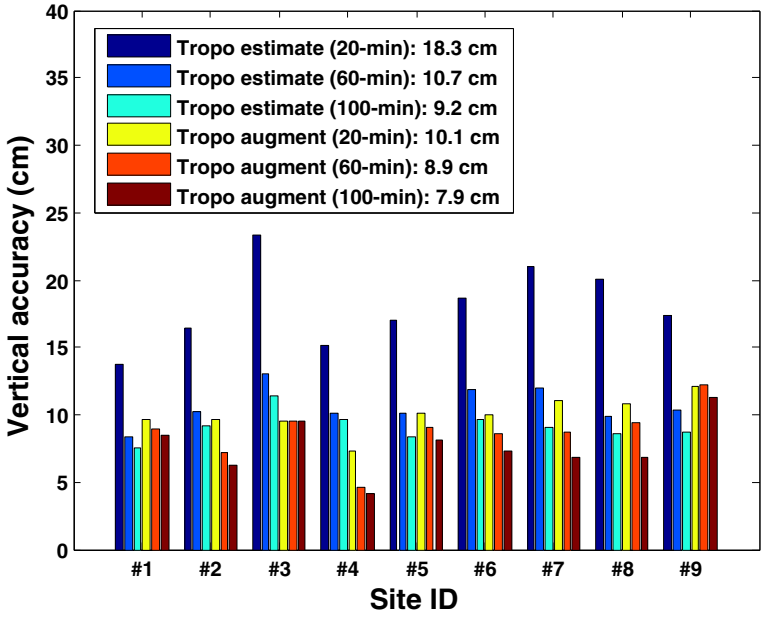

Figure 8 Vertical RMS accuracies with troposphere estimation and augmentation on DOY 127. Vertical RMS accuracies with troposphere estimation and augmentation after 20-, 60-, and 100-minute initialization periods.

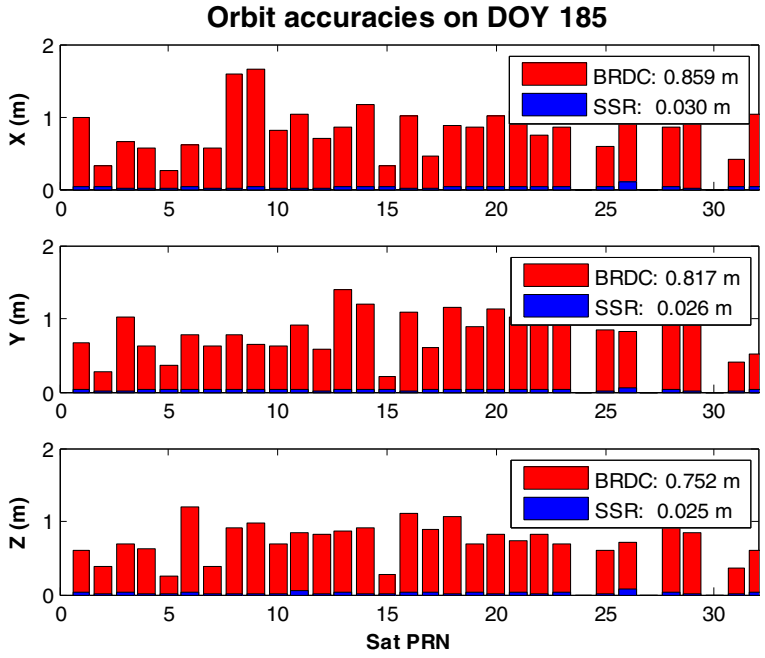

Figure 9 RMS accuracies of BRDC and SSR-corrected orbits against IGS final orbit products on DOY 2013 185.

Case study 2: active troposphere condition

The second case study describes a troposphere ZWD accumulating phase on DOY 2013 185, 1 day before a severe rainfall event on the following days. All the processing settings and strategies are the same as those used in the first case study. First, the CNES real-time orbit and clock products are analyzed with results shown in Figures 9 and 10. The overall accuracies of approximately 5 cm and 0.523 ns are obtained for satellite orbits and clock errors, respectively. Second, the precisions of local troposphere

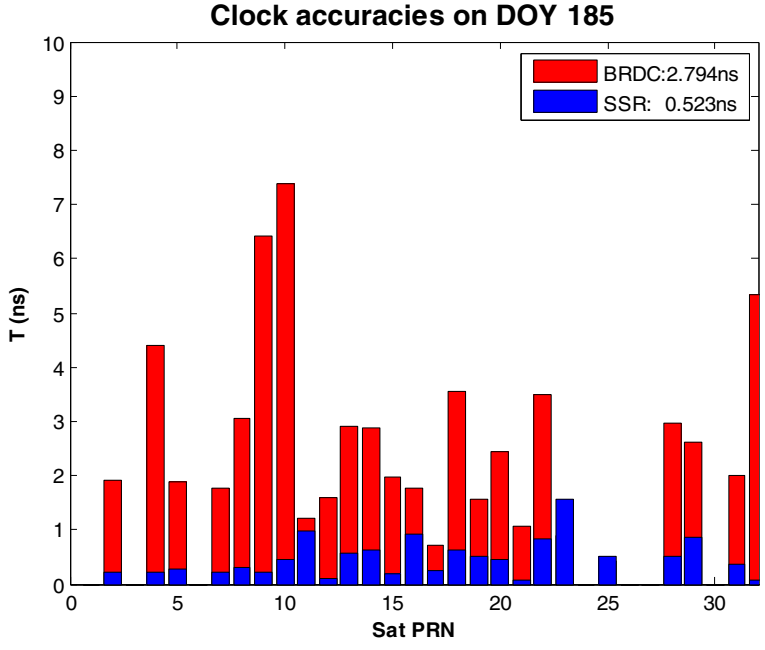

Figure 10 RMS accuracies of BRDC and SSR-corrected clocks against IGS final clock products on DOY 2013 185.

Table 3 Precisions of the local troposphere model for each station in case 2

Site	Station number									Overall
	1	2	3	4	5	6	7	8	9	
RMS (cm)	0.83	0.77	1.31	1.01	1.15	1.06	1.10	1.07	1.15	1.05

model for each station are summarized in Table 3 with an overall precision of 1.05 cm. The interpolated and estimated ZWD time series at station no. 5 are again taken as an example in Figure 11. Unlike the relatively stable pattern of the ZWD time series on DOY 127, an ascending pattern has been identified for the daily ZWD time series on DOY 185. Third, Figures 12 and 13 illustrate RMS accuracies of the horizontal and vertical coordinate solutions. Similar to the first case study, more significant improvements can be detected in the vertical component than the horizontal component. The horizontal RMS accuracies of 12.4 cm and the vertical RMS accuracies of 13.0 cm have been obtained after 20-min initialization time.

Conclusions

The IGS real-time service enables real-time PPP at a global scale. But real-time PPP is still limited by the long convergence time. In order to reduce the convergence time, this paper proposes a local troposphere augmentation method to help eliminate the troposphere effects and accelerate PPP convergence. An optimal local troposphere fitting model is proposed in this paper. The determined optimal local troposphere model is broadcast to the users, so there is no need for the user to establish communication connection to the server and no limit on the maximum number of allowed users.

The proposed method has been evaluated by a CORS network under quiet and active troposphere conditions on DOY 2013 127 and 185, respectively. First, the real-time orbit and clock corrections are assessed against the IGS final products. The results show that the current IGS CLK90 real-time stream can provide <5 cm orbit and approximately 0.5 ns clock accuracies on both days. Second, using the proposed method the optimal local troposphere model has been determined with the overall precision of 1.42 cm on DOY 127 and 1.05 cm on DOY 185. Third, the determined local troposphere model is applied to augment real-time PPP at the user end. The results indicate that real-time PPP with local troposphere augmentation can provide 9.2-cm horizontal and 10.1-cm vertical positioning accuracies after 20 min of initialization time under the quiet troposphere condition, which is a significant improvement over the 13.2-cm horizontal and 18.3-cm vertical accuracies of real-time PPP with troposphere estimation. Moreover, the horizontal accuracies of 13.0 cm and the vertical accuracies of 12.4 cm have been obtained after 20-min initialization time under the active troposphere condition, compared to the 16.0-cm horizontal and 23.4-cm vertical accuracies in the conventional troposphere estimation approach.

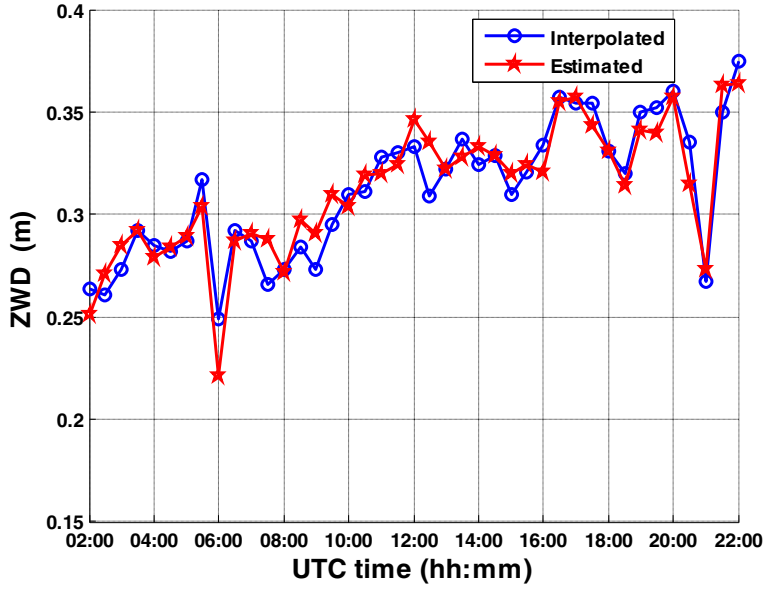

Figure 11 Interpolated and estimated ZWD at station no. 5. Interpolated (blue circle) and estimated (red star) ZWD at station no. 5 from UTC 02:00 to 22:00 on DOY 185.

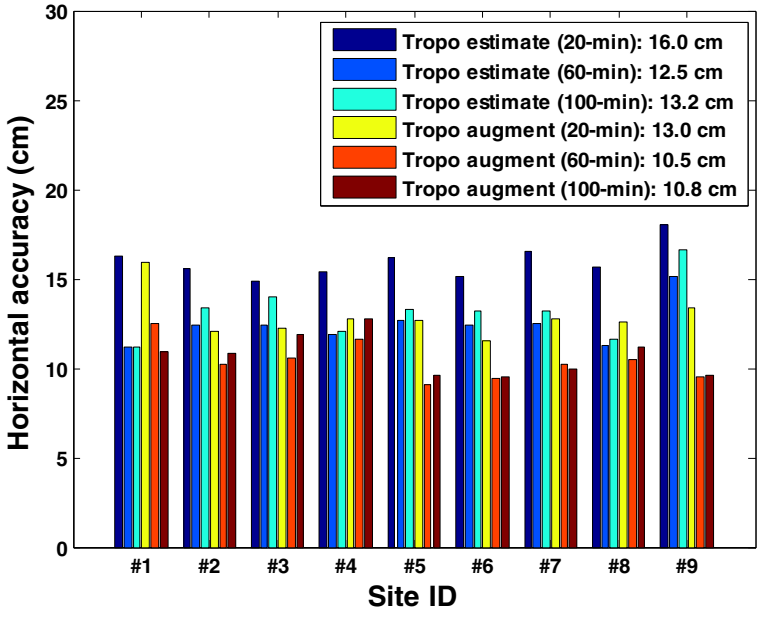

Figure 12 Horizontal RMS accuracies with troposphere estimation and augmentation on DOY 185. Horizontal RMS accuracies with troposphere estimation and augmentation after 20-, 60-, and 100-min initialization periods.

In addition to local troposphere augmentation, the ambiguity fractional bias is another limiting factor to real-time PPP. We have already demonstrated the improvement of PPP ambiguity-resolved height solution using troposphere corrections in a post-mission mode (Shi and Gao 2014). An investigation should be conducted in the future to further improve the positioning performance by considering the impacts of local troposphere augmentation on real-time PPP with integer ambiguity resolution.

So far this paper only concerns the local CORS network within a small coverage. More efforts will also be considered for the ZWD fitting model determination and transition for regional CORS networks with larger coverage in the future.

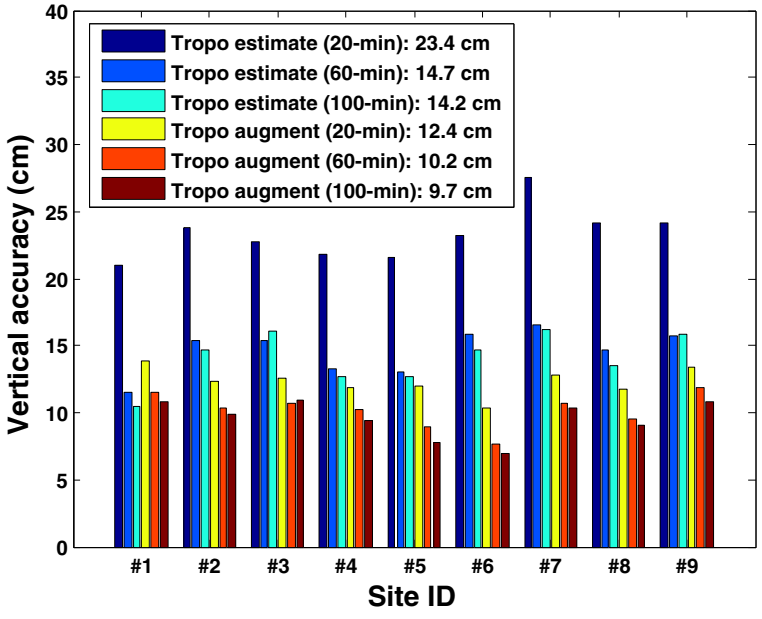

Figure 13 Vertical RMS accuracies with troposphere estimation and augmentation on DOY 185. Vertical RMS accuracies with troposphere estimation and augmentation after 20-, 60-, and 100-minute initialization periods.

Abbreviations
CORS: Continuous Operating Reference Station; DOY: day of year; GNSS: Global Navigation Satellite System; GPS: Global Positioning System; GPT: global pressure and temperature; IGS: International GNSS Service; PPP: precise point positioning; RMS: root mean square; RT: real time; RTCM: Radio Technical Commission for Maritime Services; RTPP: Real-Time Pilot Project; SOS: sum of square; SSR: space state representative; VRS: virtual reference station; ZHD: zenith hydrostatic delay; ZWD: zenith wet delay.

Competing interests
The authors declare that they have no competing interests.

Authors' contributions
SJ initiates and leads this research. XC participates in the data processing, analysis, and makes the figures. GJ organizes the group discussion and involves in drafting the manuscript. GY involves in the analysis and discussion of the results, critically revises the manuscript, and proof-reads the submission. All authors read and approved the final manuscript.

Authors' information
SJ is a lecturer of Wuhan University. His current research involves GNSS precise point positioning and GNSS meteorology. XC is a PhD candidate of Wuhan University. His current research is regional troposphere and ionosphere modeling. GJ is a professor of Wuhan University. His current research involves GNSS positioning and engineering surveying. GY is a professor of The University of Calgary. His research expertise includes both theoretical aspects and practical applications of satellite positioning and navigation systems.

Acknowledgements
IGS and CNES are acknowledged for providing the post-mission and real-time satellite precise orbit and clock products. We would like to acknowledge the anonymous reviewers and the editor for their valuable comments on this manuscript. This work has been supported by the National Key Developing Program for Basic Sciences of China (Grant No. 2012CB719902), National Natural Science Foundation of China (Grant No. 41371432), Liaoning Talent Program (Grant No. LR2011007), and Key Laboratory of Precise Engineering and Industry Surveying, National Administration of Surveying, Mapping and Geoinformation (Grant No. PF2012-13).

Author details
[1]School of Geodesy and Geomatics, Wuhan University, Wuhan 430079, China. [2]Department of Geomatics Engineering, University of Calgary, Calgary, AB T2N 1N4, Canada. [3]School of Geomatics, Liaoning Technical University, Fuxin 123000, China.

Received: 25 November 2013 Accepted: 17 April 2014
Published: 6 May 2014

References
Altiner Y, Mervart L, Neumaier P, Sohne W, Weber G (2010) Real-time PPP results from global orbit and clock corrections. Paper presented at EGU general assembly, Vienna
Alves D, Monico J (2011) GPS/VRS positioning using atmospheric modeling. GPS Solut 15(3):253–261
Boehm J, Niell A, Tregoning P, Schuh H (2006) Global Mapping Function (GMF): a new empirical mapping function based on numerical weather model data. Geophys Res Lett 33, L07304, 10.1029/2005GL025546
Boehm J, Heinkelmann R, Schuh H (2007) Short note: a global model of pressure and temperature for geodetic applications. J Geophys Res 81(2):679–683
Caissy M, Agrotis L, Weber G, Hernandez-Pajares M, Hugentobler U (2012) Coming soon: the international GNSS real-time service. www.gpsworld.com/gnss-system-augmentation-assistanceinnovation-coming-soon-13044/. Accessed 03 Jun 2013
Chen J, Li H, Wu B, Zhang Y, Wang J, Hu C (2013) Performance of real-time precise point positioning. Mar Geod 36(1):98–108
Dai L, Han S, Wang J, Rizos C (2004) Comparison of interpolation algorithms in network-based GPS techniques. Navigation 50(4):277–293
Gao Y (2005) P3 user manual. http://people.ucalgary.ca/~ygao/p3_demo.htm. Accessed 08 Jan 2013
Gao Y, Chen K (2004) Performance analysis of precise point positioning using real-time orbit and clock products. J GPS 3(1–2):95–100
Gérard P, Luzum B (2010) IERS conventions 2010. http://www.iers.org/nn_11216/SharedDocs/Publikationen/EN/IERS/Publications/tn/TechnNote36/tn36. Accessed 27 Apr 2012
Hadas T, Kaplon J, Bosy J, Sierny J, Wilgan K (2013) Near-real-time regional troposphere models for the GNSS precise point positioning technique Meas. Sci Technol 24:055003
Ibrahim H, El-Rabbany A (2011) Performance analysis of NOAA tropospheric signal delay model. Meas Sci Technol 22:115107
Kouba J (2009) A guide to using International GNSS Service (IGS) products. http://acc.igs.org/UsingIGSProductsVer21.pdf. Accessed 23 Jun 2013
Laurichesse D (2011) The CNES real-time PPP with undifferenced integer ambiguity resolution demonstrator. ION GNSS 2011, Portland, Oregon, September 2011
Li H, Chen J, Wang J, Hu C, Liu Z (2010) Network based real-time precise point positioning. Adv Space Res 46:1218–1224
Li X, Zhang X, Ge M (2011) Regional reference network augmented precise point positioning for instantaneous ambiguity resolution. J Geophys Res 2011(85):151–158
RTCM Special Committee 104 (2011) Differential GNSS (Global Navigation Satellite Systems) services - version 3 + amendments 1, 2, 3, 4, and 5 to RTCM 10403.1. http://ssl29.pair.com/dmarkle/puborder.php?show=3. Accessed 03 Jun 2013
Shi J, Gao Y (2014) A troposphere constraint method to improve PPP ambiguity-resolved height solution. J Navigat 67(2):249–262
Sturze A, Mervart L, Sohne W, Weber G, Wübbena G (2012) Real-time PPP using open CORS networks and RTCM standards. Paper presented at PPP-RTK symposium, Frankfurt, Germany, 12–13 March 2012
Tao W (2008) Near real-time GPS PPP-inferred water vapor system development and evaluation. Master Thesis, Department of Geomatics Engineering, University of Calgary, University of Calgary, UCGE Report 20275, 2008
Wang M, Chai H, Xie K, Chen Y (2013) PWV inversion based on CNES real-time orbits and clocks. J Geod and Geodyn 33(1):137–140
Xiong Y, Huang D, Ding X, Yin H (2006) Research on the modeling of tropospheric delay in virtual reference stations. Acta Geodaetica et Cartographic Sinica 35(5):118–121
Zhang X, Zhu F, Li P, Zhai G (2013) Zenith troposphere delay interpolation model for regional CORS network augmented PPP. Geomatics Inf Sci Wuhan Univ 38(6):679–683

doi:10.1186/1880-5981-66-30
Cite this article as: Shi *et al.*: Local troposphere augmentation for real-time precise point positioning. *Earth, Planets and Space* 2014 **66**:30.